



HAL
open science

Kinetics of corrosion propagation in reinforced concrete contaminated with chlorides

V. Bouteiller, V. L'Hostis, E. Marie-Victoire, J. Schneider, F. Boinski, C. Cremona

► **To cite this version:**

V. Bouteiller, V. L'Hostis, E. Marie-Victoire, J. Schneider, F. Boinski, et al.. Kinetics of corrosion propagation in reinforced concrete contaminated with chlorides. ICDC 2014 - 2nd International Congress on Durability of Concrete, Dec 2014, New Delhi, India. cea-02509084

HAL Id: cea-02509084

<https://cea.hal.science/cea-02509084>

Submitted on 16 Mar 2020

HAL is a multi-disciplinary open access archive for the deposit and dissemination of scientific research documents, whether they are published or not. The documents may come from teaching and research institutions in France or abroad, or from public or private research centers.

L'archive ouverte pluridisciplinaire **HAL**, est destinée au dépôt et à la diffusion de documents scientifiques de niveau recherche, publiés ou non, émanant des établissements d'enseignement et de recherche français ou étrangers, des laboratoires publics ou privés.

KINETICS OF CORROSION PROPAGATION IN REINFORCED CONCRETE CONTAMINATED WITH CHLORIDES

Véronique Bouteiller ¹, Valérie L'Hostis ², Elisabeth Marie-Victoire ³, Julien Schneider ⁴, Frédéric Boinski ⁴ and Christian Cremona ⁵

¹ Université Paris Est, IFSTTAR, Département Matériaux et Structures, Laboratoire Sécurité et Durabilité des Ouvrages d'Art, Champs sur Marne, France

² CEA Saclay, CEA, DEN, DPC, SECR, Laboratoire d'Etude du Comportement des Bétons et des Argiles, Gif-sur-Yvette, France

³ Laboratoire de Recherche des Monuments Historiques, LRMH, CNRS-USR 3224, Champs-sur-Marne, France

⁴ CEREMA, DTer, Ile de France, Laboratoire Eco-Matériaux, Chimie et Matériaux Ouvrages d'Art, France

⁵ CEREMA, Technical Center for Bridge engineering, Sétra, Sourduin, France

Abstract

Rebar corrosion of reinforced concrete is the main cause of deterioration of structures such as bridges, piers, monuments, etc.... Considering the amount of structures built using reinforced concrete all along the 20th century, monitoring and control of reinforcement bear a significant practical importance in durability assessment.

The aim of this paper is (i) to study the corrosion kinetics of reinforced concrete structures in the propagation phase in order to ascertain the corrosion process versus time and (ii) to propose a prediction for reinforced concrete structure durability based on steel thickness loss.

In the aim of improving corrosion comprehension and prediction, within the French national project APPLLET, reinforced concrete slabs, polluted by chlorides (mix or wetting/drying cycles) were exposed to outdoor environmental conditions as well as to controlled temperature and relative humidity conditions during a three years period.

Corrosion of reinforcement was monitored four times per year by the means of three measurements (half-cell potential, electrochemical impedance spectroscopy and linear polarization resistance) and then, corrosion current density was calculated. Destructive analyses of the steel/concrete interface were also conducted in order to determine the steel loss by gravimetry and the nature of the oxide species by Raman microspectroscopy.

Results show that in order to accurately predict the durability of reinforced concretes, measurements need to be performed regularly because the corrosion rate is an instantaneous value that fluctuates with time. Concerning the kinetics of the corrosion propagation phase for chlorinated concretes, the data analysis evidenced that steel thickness loss versus time follows a power law rather than a linear law. Moreover, the occurrence of cracks was related to the steel loss versus time. Finally, the steel loss obtained on samples exposed to outdoor conditions was relatively close to the one observed on samples exposed to controlled conditions.

1. INTRODUCTION

Reinforced concrete is a composite engineering material widely used in construction industry (buildings, bridges, tunnels, nuclear plants, historical monuments, etc). One of the major factors responsible for the deterioration of these structures is the corrosion of the reinforcement [1-6] which may result in damages in the form of cracking and spalling of the concrete cover. In addition, the

structural damage may consist in loss of bond between reinforcement and concrete and loss of reinforcement cross-sectional area, resulting in loss of serviceability and structure safety.

Initiation of corrosion is generally associated with the loss of protective action provided by the concrete cover to the reinforcement when in contact with aggressive agents (pollutants). This effect which is related to a transfer / transport approach and which has been extensively studied on concrete samples (with no reinforcement) states that corrosion occurs when:

- The carbonation front has reached the rebar level and the concrete pH has decreased from almost 13 to 9. Then, steel passivity is no more sustained.
- The chloride ions from the external environment have penetrated into the concrete matrix to reach the steel rebar in concentrations high enough to break down the passive layer.

Models that correlate the penetration of pollutants and corrosion, whatever their nature (empirical, deterministic, analytical or probabilistic) [7-9] would gain in reliability if they could be calibrated by electrochemical studies performed on *reinforced* concrete samples. Up to now, only a few papers on the corrosion of reinforcement in concrete versus time are available [10-14].

Propagation of corrosion is not well documented. Li [15] stated that: "since it is the effects of reinforcement corrosion that damage the structural resistance, more research on corrosion propagation in particular, experimental research, is necessary to develop rational models used in whole life performance assessment for corrosion-affected concrete structures".

Regarding inspection, repair, strengthening, replacement and demolition of the age-degraded reinforced concrete structures, qualitative and quantitative data are also needed and therefore monitoring and control of reinforcement corrosion [16] bear a significant practical importance.

This paper focuses on the corrosion propagation phase in reinforced concrete structures, topic explored within the frame of the French national project APPLET, which main aim was to study the corrosion kinetics of reinforced concrete structures in order to ascertain the corrosion process versus time. Three series of reinforced concrete samples were studied: two chloride contaminations (chlorides in the mix or chlorides that have penetrated by wetting/drying cycles) and one sound concrete reference. Each series were exposed to six different controlled environmental conditions based on two temperatures (25 and 45 °C) and three relative humidities (60, 80 and 92%) and also to the outdoor climate. Corrosion evolution was monitored four times a year over a three year period by non-destructive electrochemical techniques such as half-cell potential, impedance spectroscopy and linear polarisation resistance. Then, corrosion current density was calculated. Finally, destructive analysis of the steel/concrete interface for some samples provided additional information.

2. MATERIALS AND METHODS

2.1. Specimens

Reinforced concrete specimens were prisms (which dimensions were 150x50x50 mm) that contained a central rebar (6 mm diameter) with an uninsulated steel surface equal to 18.8 cm². These prisms were sawed from reinforced concrete slabs after the process of ageing. More details can be found in [17].

2.2. Concrete states

Three concrete states were studied: Prisms "T" were sound reinforced concrete (used as reference). Prisms "G" were contaminated with 5% of NaCl by weight of cement added in the mix. Prisms "I" contained chlorides that have penetrated by wetting and drying cycles (salted pond NaCl 35g/L). For the two states of chloride contamination, the chloride content was higher than 0.4% by weight of cement (this ratio usually refers to a condition for which corrosion is likely to occur [18]).

2.3. Environmental conditions

Six controlled environmental conditions were considered based on two temperatures (20°C and 45°C) and three relative humidities (60%, 80% and 92%). The outdoor condition was the suburb of Paris where temperatures (-10 to +29°C), relative humidity (29 to 91%) and precipitations (0 to 4 cm) recorded from September 2008 to December 2011 were coherent with the French climate (except for the high precipitations in December 2009 (12 cm)).

2.4. Measurement termed points

Corrosion rebar characterizations were carried out 4 times a year from 2008 to 2011 except for 45°C and 80%RH where measurements were stopped approximately after 2 years because of the excessive cracking of the prisms. Measurement termed points and their corresponding dates are indicated in Table 1.

Table 1 - Measurement termed points

Label	E00	E01	E02	E03	E04	E05	E06	E07	E08	E09	E10	E11	E12
Date	Sep 2008	Dec 2008	April 2009	June 2009	Sept 2009	Jan 2010	April 2010	June 2010	Sept 2010	Jan 2011	June 2011	Sept 2011	Dec 2011
Months	0	3	6	9	12	15	18	21	24	27	30	33	36

2.5. Visual inspections of prisms to follow the corrosion process

A visual inspection of each prism was carried out with time to ascertain corrosion signs such as rust spots, rust leaching, cracks or spallings. Pictures were taken and comments were added to the database.

2.6. Electrochemical tests

For a steel reinforcing bar in concrete, a simple equivalent electronic circuit, known as Randle's circuit [19] can be considered to model the corrosion interface. In this model, the corroding surface of steel is often considered as a charge transfer resistance (R_p) in parallel with a double layer capacitance which is provided by charged ions on the surface of the steel. The resistance R_e represents the electrical resistance of the concrete cover together with the electrolyte between the rebar and the surface.

In order to calculate the corrosion current density or corrosion rate i_{corr} of the prism rebar, three non-destructive techniques were used: half cell potential (E_{corr}) monitoring, electrochemical impedance spectroscopy (EIS) and linear polarization resistance (LPR). These tests were undertaken 4 times a year over a three year period. The measurements were conducted using a multichannel Bio-Logic potentiostat (VMP2Z model) and the EC-Lab 10.12 software. For the sound concrete prisms T a low current capability was used because the current values were in the nanoAmpere range.

The corrosion current density i_{corr} ($\mu\text{A}/\text{cm}^2$) also named corrosion rate was then calculated from the Stern and Geary equation [20] : $i_{\text{corr}} = B/R_p.S$ where B is a constant (26 or 52 mV [21], R_p the polarization resistance (ohm) and S the steel surface (18.8cm² in this study)). As the frontier between passive and active corrosion is not known the B value was always chosen equal to 26 mV.

A database gathered all the measured and calculated values [17].

For each concrete state (T, G and I) corrosion current density was calculated as the average of the five prisms per environmental conditions (or less if autopsy or cracked prisms) and analysed considering the four levels of corrosion proposed by the RILEM [22]: negligible ($i_{\text{corr}} < 0.1 \mu\text{A}/\text{cm}^2$), low (0.1-0.5 $\mu\text{A}/\text{cm}^2$), moderate (0.5-1 $\mu\text{A}/\text{cm}^2$) and high ($i_{\text{corr}} > 1 \mu\text{A}/\text{cm}^2$).

2.7. Examinations of steel/concrete interface by destructive analysis

Destructive examinations of steel/concrete interface was realised on prisms after 15 or 21 months (Table 2). Each prism was cut into two parts: one for gravimetric measurements and the second one for the surface analysis.

Table 2 - Prisms for autopsy

Environmental conditions	Time (months)	T prisms	G prisms	I prisms
20°C, 92%RH	15		633	660
	21	592	625	652
45°C, 92%RH	15		632	662
	21	595	613	673
Outdoor conditions	21	600	614	658

2.7.1. Gravimetric measurements

After separating the rebar from the cement matrix, corrosion products were removed from the steel surface using the procedure detailed in [23]. The difference between initial mass (estimated from the reinforcement geometry and iron density) and final one (weighted after removing corrosion products) gave the steel mass loss. Knowing the mass loss the average corrosion rate for the duration of the test was calculated assuming a homogeneous corrosion pattern.

2.7.2. Surface analysis

The sample was cut transversally in order to observe the steel/concrete interface. It was then mounted in epoxy resin at room temperature. Transverse sections were performed under ethanol lubricant. The surface of the transverse section was prepared by polishing under ethanol, first by SiC (grade 80 to 4000) and finishing with diamond paste (3 μm). The steel/concrete interface was then observed by optical microscopy to determine the morphology of the corrosion layers (generalised or localised corrosion). For several locations around the sample, the thickness of the corroded layer were recorded (around 50 points per sample section).

In order to identify the nature of the corrosion products at the steel/concrete interface, analyses by Raman microspectroscopy were performed at the LADIR (Laboratoire de Dynamique Interaction et Réactivité – UMR 7075) on the polished cross sections. A Jobin Yvon-Horiba LabRam Infinity spectrometer equipped with a frequency-doubled Nd:YAG Laser at 532 nm was used. Spectral resolution of this set-up was about 2 cm^{-1} . Micro-measurements were realised with a x100 long-focus Leitz objective which gave a beam waist diameter of about 1.5 μm . Excitation Laser power on sample was filtered at least below 0.1 mW in order to avoid thermal effect for sensitive iron oxides and oxyhydroxides. The phases were identified by comparison with powder standards given by earlier publications [24].

3. RESULTS AND DISCUSSION

3.1. Visual inspections of reinforced prisms

Concerning sound concrete T prisms, no sign of corrosion was detected during the three year study whatever the environmental temperature and relative humidity conditions.

At 20°C, no visible sign of corrosion was detected on G prisms and only one I prism out of 5 showed some rust and small cracks after 21 months.

Increasing temperature to 45°C, leads to higher degradations particularly for relative humidity of 80% and 92%. At 45°C and 80%RH, after 12-18 months the G prisms were so badly corroded that they had transformed into a 2-way split prism or even puzzles. For I prisms, this same state of degradation was observed with some delay (after 18-21 months). At 45°C and 92%RH, cracks began to occur after 6 months on one out of five G prisms and after 9 months on four G prisms. After 15 months a complete loss of bond between steel and concrete was observed. For the same environmental condition, corrosion signs for prisms I appeared later on compared to G prisms: first visual corrosion signs were seen after 15 months for one prism (673 which has been autopsied). Picture 1 illustrates the complete evolution of the corrosion signs for one I prism versus time: rust was observed after 21 and 24 months. Then a longitudinal crack occurred after 27 months. Finally, at 30 months, there was a complete loss of bond between steel and concrete.



21 months 24 months 27 months 30 months
 Picture 1 - Evolution of corrosion signs on one I prism exposed to 25°C and 92%RH (689) and exposed to 45°C and 92%RH (679).

For prisms stored outdoor, visible sign of corrosion was noticed on one I prism out of 5 after 21 months and one G prism out of 5 after 24 months.

3.2. Instantaneous corrosion current density

Corrosion current density values versus the measurement termed points together with the corrosion levels from the Rilem [22] are presented in Figure 1 for specimens exposed to controlled environmental conditions and in Figure 2 for those exposed to outdoor conditions.

Sound reinforced concrete T remained passive (i_{corr} values below $0.01 \mu A/cm^2$) through the three year study whatever the environmental conditions.

Chloride contaminated reinforced concretes (G and I) were corroding for relative humidities higher than 60%. This result shows that the corrosion process does not only respond to a chloride content but also to an environmental condition and these two parameters need to be considered together. At 20°C, moderate and high levels of corrosion were observed for 80 and 92% RH. At a higher temperature equal to 45°C, the i_{corr} values were in the range of high corrosion level and after 12 months for G prisms and after 15 months for I prisms, the measurements were no more possible because of the cracks.

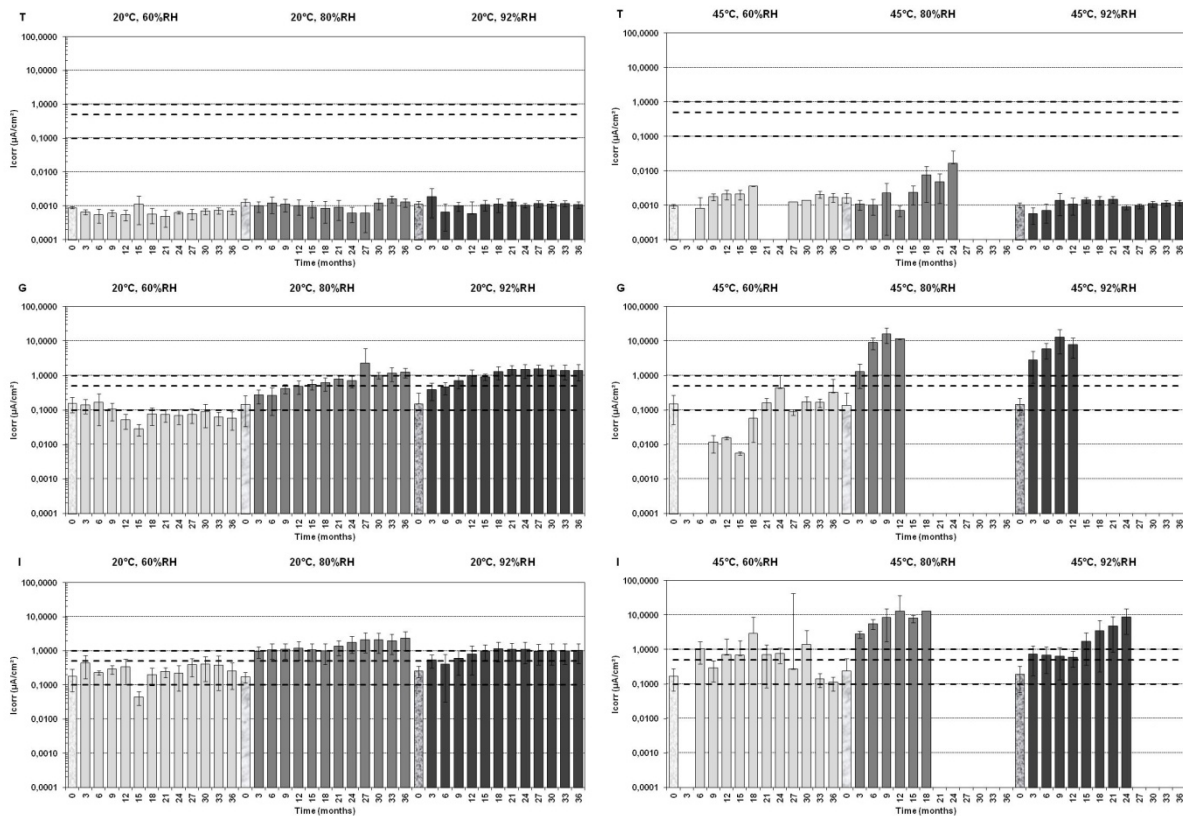


Figure 1 - Corrosion current density values, i_{corr} , versus measurement termed points, depending on concrete states (T, G and I) and on environmental conditions.

Corrosion current density values obtained for outdoor environmental conditions (Figure 2) were in the moderate to high corrosion levels. They showed some fluctuations depending on the measurement termed points that can be explained by the climate changes. Studies in outdoor conditions have

demonstrated as general trends that corrosion results usually follow the day/night cycles or the year-seasonal cycles, sheltered or unsheltered conditions [25]. The influence of a rain event has also been mentioned [26].

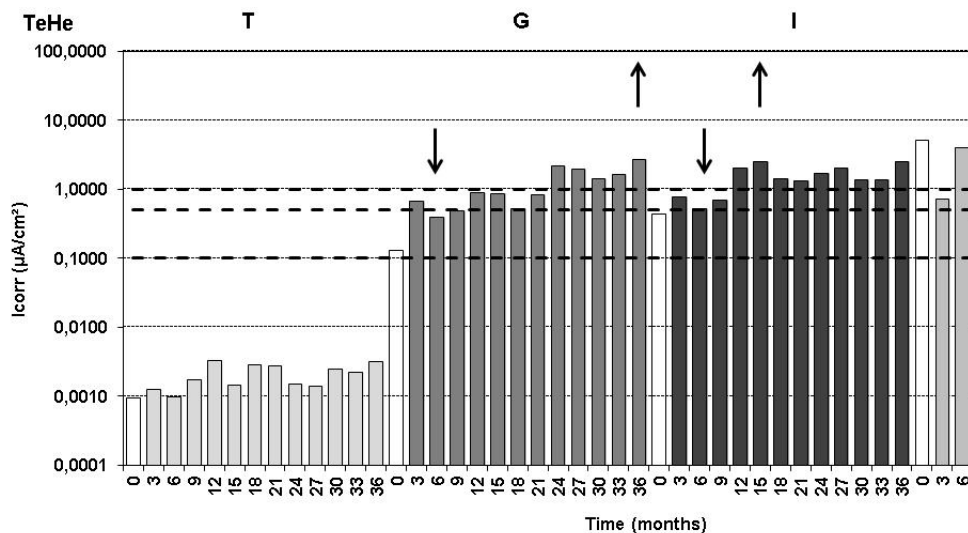


Figure 2 - Corrosion current values in a log scale for the reinforced concrete prisms (T, I, and G) exposed to outdoor conditions versus time. (Arrows indicate the minimum and the maximum values for each concrete state).

3.3. Kinetics of corrosion

Corrosion current density evaluation, most commonly named corrosion rate, is the key parameter used for determining the rate of deterioration and for quantitatively predicting the remaining service life of reinforced concrete structures. Then corrosion current density can be transformed in steel weight loss using the Faraday's law. Knowing the mass loss, the steel thickness loss which is more useful for civil engineering calculations, can then be calculated. It is to be mentioned that steel thickness loss is different from corrosion product thickness because depending on the level of oxidation, the volume of the iron oxides may be up to about 6.5 times the original iron volume [27].

Kinetics of the corrosion in its propagation phase was expressed as the steel thickness loss versus time. Calculations of the steel thickness loss (in μm) from the experimental data were performed considering:

- time equal to zero was not considered,
- time in between two measurement termed points (which could be slightly less or more than three months) was calculated in seconds,
- for each time period, the considered i_{CORR} was the mean of the values determined before and after the measurement termed points.

Knowing that the i_{CORR} is an instantaneous value, the discrepancy that could result in the durability prediction was studied considering (i) the minimum value of i_{CORR} ; (ii) the maximum value of i_{CORR} and (iii) the whole set of measured i_{CORR} values (transformed into thickness loss). This in turn will state if a linear kinetic law assumption (that is usually considered) is accurate or not.

Figure 3 presents the steel thickness loss versus time for the reinforced concretes I considering a linear law (at) or a power law (ct^α) to fit the experimental data (equation and correlation factor appear on graphs). When considering a linear law, curves based on the minimum and on the maximum values of i_{CORR} were added on the graph.

From this graph, firstly, it was obvious that the discrepancy could be very important considering a linear law of corrosion (for example, for I prisms after three years: thickness steel loss was almost equal to 20, 50, 90 μm considering the minimum value, the whole set of measurements or the maximum value of i_{CORR}). Of course this discrepancy increases with longer time. Secondly, the mathematical power law fitted more accurately the corrosion propagation process than the linear law.

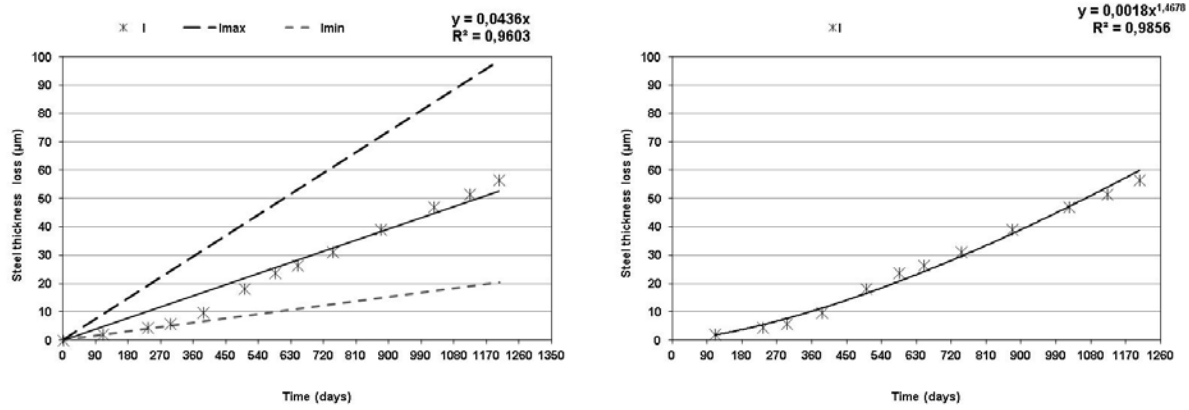


Figure 3 - Steel thickness loss of I prisms exposed to outdoor conditions versus time for predicting durability (left: linear law; right: power law).

Table 3 presents the mathematical power law (steel thickness loss versus time) for the corrosion propagation phase depending on the type of chloride contamination and on the environmental conditions.

For G prisms exposed to outdoor conditions, similar results as for I prisms were found.

For prisms exposed to controlled environmental conditions, for 20°C and 60%RH, the α value was lower than 1 probably because of a lack of humidity. Otherwise, the α value was higher than 1 which probably means that once the corrosion is in the propagation phase, corrosion increases like in a catalytic process. The α value also increased with temperature.

This study is still ongoing and future results will be useful to confirm that the proposed mathematical power law correctly describes the corrosion propagation kinetics for longer times.

Table 3 – Mathematical law of the corrosion propagation phase (steel thickness loss = ct^α)

Prisms		c	α	R ²						
I	Outdoor	1,80E-3	1,47	0,99						
G	Outdoor	1,10E-3	1,47	0,98						
Prisms	Relative humidity Temperature	60%			80%			92%		
		c	α	R ²	c	α	R ²	c	α	R ²
I	20°C	1,41E-2	0,93	0,99	3,70E-3	1,35	1,00	2,00E-3	1,37	1,00
	45°C	1,00E-4	1,82	0,97	7,00E-4	1,91	1,00	7,00E-5	2,13	0,95
G	20°C	2,14E-2	0,71	0,98	3,00E-4	1,62	0,98	4,00E-4	1,63	1,00
	45°C	2,00E-4	1,34	0,74	2,00E-5	2,59	0,97	7,00E-4	1,92	0,99

3.4. Comparison of the steel thickness loss of prisms exposed to outdoor or to controlled environmental conditions.

Figure 4 presents the thickness loss results of I prisms obtained for the outdoor condition together with the results obtained for the three controlled environmental conditions based on a 20°C temperature. Similarly, Figure 5 presents the results for G prisms. It can be observed that corrosion process of I prisms stored in outdoor conditions was relatively close to the controlled environmental conditions of 20°C and 80% RH. Concerning G prisms, the outdoor corrosion process was very close the one obtained for the environmental conditions of 20°C and 92% RH.

Therefore, results obtained under controlled parameter could be used as "abacus" to predict the corrosion process in outdoor conditions.

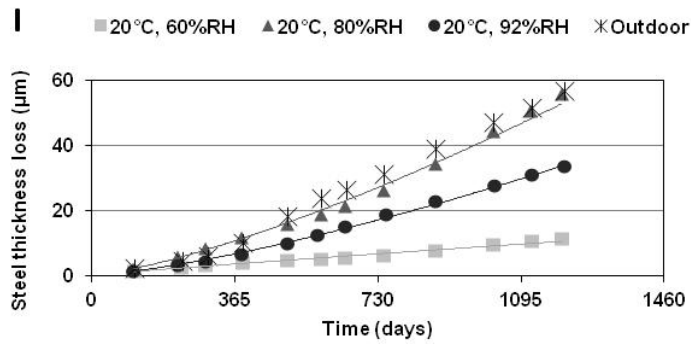


Figure 4 - Comparison of thickness loss obtained on I prisms exposed to outdoor conditions with those obtained under controlled environmental conditions.

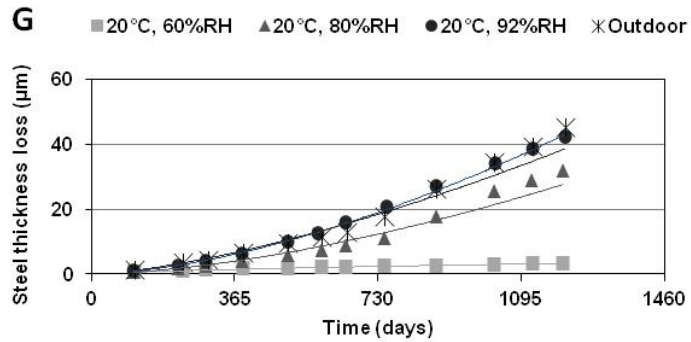
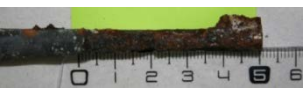


Figure 5 - Comparison of thickness loss obtained on G prisms exposed to outdoor conditions with those obtained under controlled environmental conditions.

3.5. Autopsy

Picture 2 gathers the corrosion morphology of rebars extracted from the concretes. Active corrosion of steel was highlighted when the rebars were embedded in prisms containing chlorides (G and I) for all environmental conditions (20°C, 92%RH; 45°C, 92%RH and outdoor) and both test durations (15 and 21 months). Steel rebar of the reference concrete T remained as clean as it was before sample fabrication.

Environmental conditions	Time Months	T prisms	G prisms	I prisms
20°C, 92%RH	15		 633	 660
	21	 592	 625	 652
45°C, 92%RH	15		 632	 662
	21	 595	 613	 673
Outdoor conditions	21	- 600	 614	 658

Picture 2 - Corrosion morphology of rebars extracted from concrete samples.

Results of destructive analyses are indicated in Table 4 (20°C, 92%RH conditions), Table 5 (45°C, 92%RH) and in Table 6 (outdoor conditions).

Table 4 - Destructive characterization results for the prisms exposed to 20°C and 92% RH.

Prism	Concrete state	Months	Gravimetry		Corrosion products		
			Steel thickness (μm)	V _{corr} (μm/y)	Thickness max (μm)	Thickness min (μm)	Nature of corrosion species (Raman microspectroscopy)
633	G	15	53	42	58	45	badly crystallized phases Iron oxihydroxides
625	G	21	27	15	58	0	badly crystallized phases Magnetite (iron oxide)
660	I	15	17	14	529	0	badly crystallized phases
652	I	21	33	19	0	0	Not analysed

Table 5 - Destructive characterization results for the prisms exposed to 45°C and 92% RH.

Prism	Concrete state	Months	Gravimetry		Corrosion products		
			Steel thickness (μm)	V _{corr} (μm/y)	Thickness max (μm)	Thickness min (μm)	Nature of corrosion species (Raman microspectroscopy)
632	G	15	186	149	1755	613	badly crystallized phases Iron oxihydroxides
613	G	21	368	210	1378	277	badly crystallized phases Iron oxihydroxides
662	I	15	19	15	64	0	Iron oxides
673	I	21	438	250	961	822	badly crystallized phases Iron oxihydroxides Magnetite (iron oxide)

Table 6 - Destructive characterization results for the prisms exposed outdoor.

Prism	Concrete state	Months	Gravimetry		Corrosion products		
			Steel thickness (μm)	V _{corr} (μm/y)	Thickness max (μm)	Thickness min (μm)	Nature of corrosion species (Raman microspectroscopy)
614	G	21	12	7	126	0	Magnetite / Goethite / Lépidocrocite
658	I	21	11	6	202	0	Magnetite / Ferrihydrite / Goethite

From the gravimetry analysis, steel thickness loss and average corrosion rates were in good agreement. Taking into account the precision of this kind of measurement, the duration of active corrosion from 15 months to 21 months did not clearly changed the values. The comparison of steel thickness loss obtained from gravimetry or from the mathematical law show consistent results (except for I prism exposed to 45°C and 92%RH 21 months) (Figure 6).

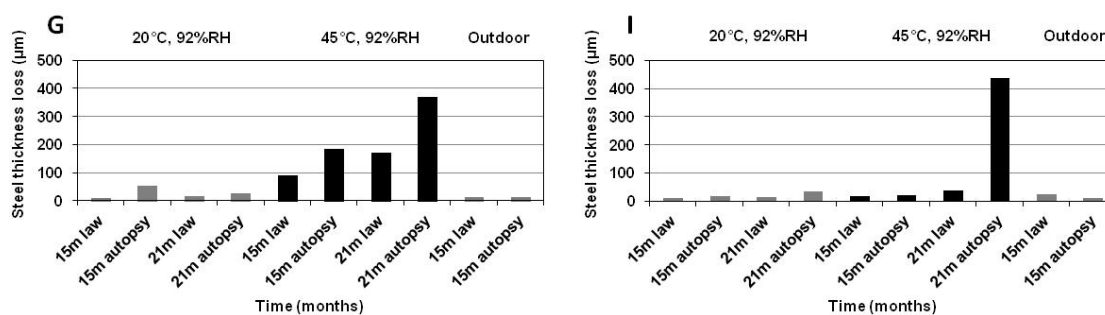


Figure 6 – Comparison of steel thickness loss determined by the mathematical law or by gravimetry.

From the analysis of corrosion products, values of maximum and minimum thicknesses were very different for the chloride contaminated concrete and were indicative of localised corrosion. Conclusions drawn for average corrosion rates can be extended for corrosion layers thicknesses. No extension of corrosion layer was noticed between 15 and 21 months of active corrosion.

Concerning corrosion products, iron oxides and oxi-hydroxides that are classically characterized on reinforced concrete structures were identified by Raman Spectroscopy (Figure 7, Figure 8 and Figure 9). Corrosion products formed in chloride contaminated concretes contained badly crystallized phases as well as other iron oxi-hydroxides (goethite and lepidocrocite). Magnetite, goethite and also ferrihydrite were identified by Neff *et al.* [28] in pits formed during chloride-induced-corrosion in concretes containing 4% (in weight) of chlorides added to the mixing water. The same result has been obtained by L'Hostis *et al.* [29] in samples containing several chloride contents added to the mixing water after 1,5 year.

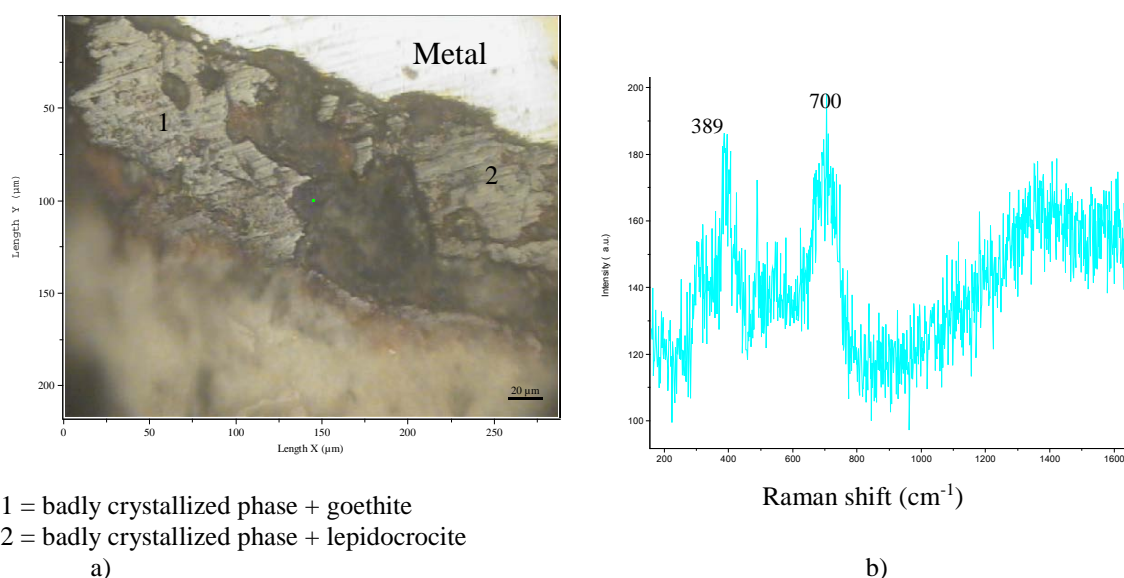


Figure 7 - (a) Examination for Micro Raman Spectroscopy of 633-G sample exposed to 20°C, 92%RH, (b) Representative Raman spectrum obtained on point 1 (identified as badly crystallized phase + goethite).

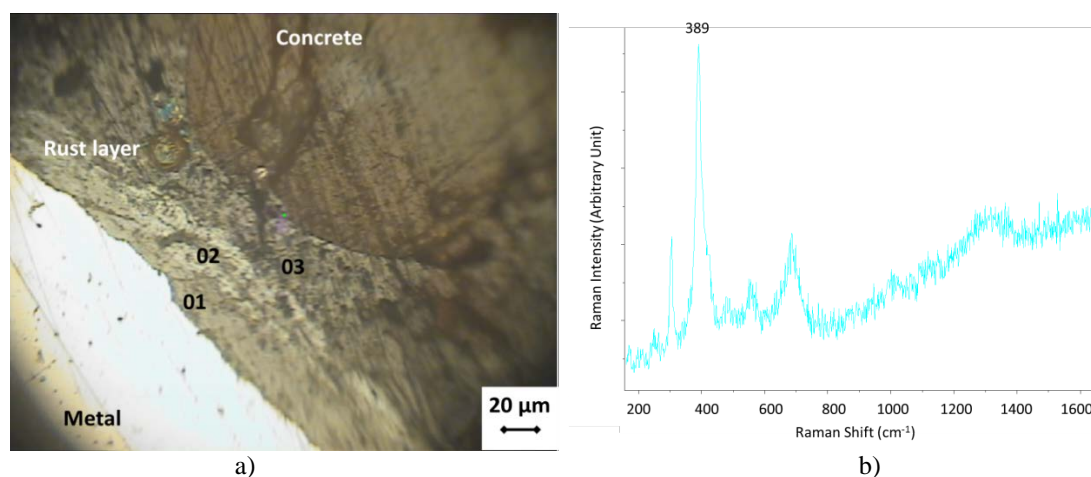


Figure 8 - a) Macrograph of the metal-interface of 658-I sample exposed to outdoor conditions. Iron oxides identified were 01: goethite, 02: magnetite, 03: ferrihydrite, b) Raman spectrum of goethite (point 01).

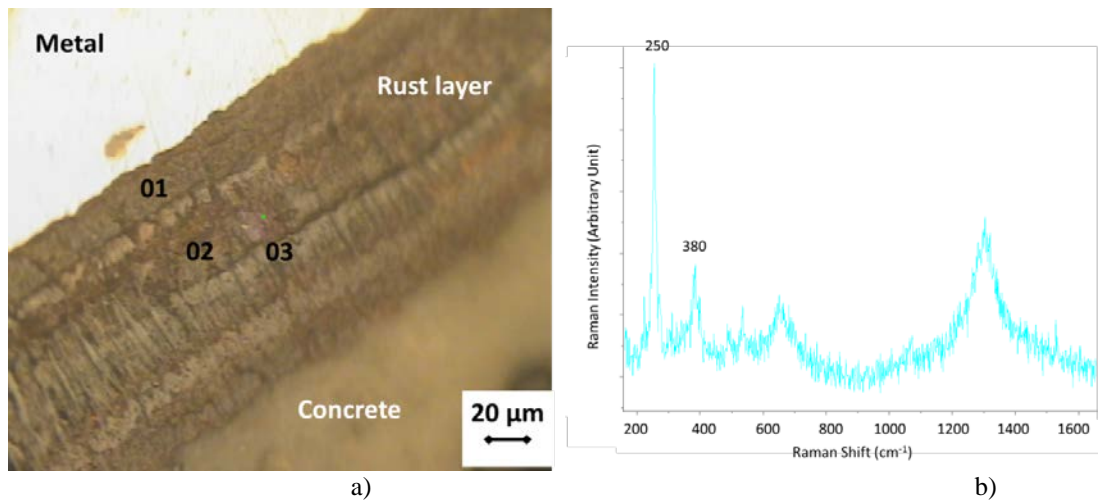


Figure 9 - a) Macrograph of the metal-interface of 614-G sample exposed to outdoor conditions. Iron oxides identified were 01: mix of goethite and ferrihydrite, 02: mix of magnetite and goethite, 03: lepidocrocite, b) Raman spectrum of lepidocrocite (point 03).

4. CONCLUSIONS and outlooks

Within the French project APPLLET, corrosion propagation of chloride (mix or wetting/drying) contaminated reinforced concrete exposed to various environmental conditions (temperature 20°C, 45°C, outdoor; relative humidity 60%, 80%, 92% and outdoor) have been studied. Reinforcement corrosion was described based on visual inspections, frequent electrochemical tests (4 times per year during 3 years), instantaneous corrosion rates, and destructive analysis. All these results with time have been gathered in a database available for the scientific community.

The results highlights that considering only one corrosion rate value and a linear law of corrosion can lead to severe discrepancies in the prediction of the corrosion kinetics ie the steel thickness loss versus time. Therefore, performing frequent measurements or even monitoring the electrochemical tests to calculate instantaneous corrosion rate is mandatory to accurately predict the reinforced concrete corrosion. Results showed that a mathematical power law better fitted the experimental values than a linear law. The power alpha value being higher than one seems to reflect that the corrosion is a likely catalytic process. However the proposed power law is representative of the behaviour of the reinforced concrete before highly cracking and cannot be used to describe the entire service life of the structure.

Moreover, results obtained outdoor were quite similar to those obtained in controlled conditions and therefore abacus could be proposed.

Finally, steel thicknesses determined by autopsy or by the mathematical law were in good agreement. Further results will confirm for a longer period of time the proposed power law relevance.

ACKNOWLEDGEMENT

The authors would like to thank G. Biadala (from LR Lille), F. Boinski and J. Schneider (from LREP Melun) for the fabrication and the ageing of the reinforced concrete slabs. They also thank E. Amblard and C. Emptaz (from CEA) for the autopsies and J. Dauthuille, A. Deman, J-F. Cherrier and U. Iftikhar (from IFSTTAR) for the electrochemical measurements. B. Koubi is also thanked for the macro development. C. Paris and L. Bellot-Gurlet are warmly acknowledged for their support in Raman spectroscopy analyses. Finally, C. Andrade from IETcc in Spain is particularly acknowledged for helpful scientific discussions and also for being part of this national project as special partner.

Investigations and results reported herein were supported from 2007 to 2010 by the National Research Agency (France) within the APPLLET research program (grant ANR-06-RGCU-001-01) and from 2010 to 2011 by Ifsttar and LRMH.

REFERENCES

- [1] G.P. Tilly, J. Jacobs, CONREPNET - Concrete repairs - Performance in service and current practice, IHS BRE Press, United Kingdom, 2007.
- [2] A. Bentur, S. Diamond, N.S. Berke, Steel corrosion in concrete - Fundamentals and civil engineering practice, E&FN SPON, London, United Kingdom, 1997.
- [3] J.P. Broomfield, Corrosion of steel in concrete - Understanding, investigation and repair, E&FN SPN, London, 1997.
- [4] L. Bertolini, B. Elsener, P. Pedferri, R. Polder, Corrosion of steel in concrete: prevention, diagnosis, repair, Wiley Vch Verlagsgesellschaft Mbh, Weinheim, 2004.
- [5] S. Audisio, G. Béranger, V. Bouteiller, Anticorrosion et durabilité dans le bâtiment, le génie civil et les ouvrages industriels ; Chapitre 18 Les traitements électrochimiques pour la réhabilitation du béton armé dégradé. , Presses Polytechniques et Universitaires Romandes ed., 2010.
- [6] A. Raharinaivo, G. Arliguie, T. Chaussadent, G. Grimaldi, V. Pollet, G. Tache, La corrosion et la protection des aciers dans le béton, Presses de l'école nationale des Ponts et Chaussées, Paris, 1998.
- [7] F. Biondini, D.M. Frangopol, Lifetime reliability-based optimization of reinforced concrete cross-sections under corrosion, *Structural Safety*, 31 (2009) 483-489.
- [8] H.-W. Song, S.-W. Pack, K.Y. Ann, Probabilistic assessment to predict the time to corrosion of steel in reinforced concrete tunnel box exposed to sea water, *Construction and Building Materials*, 23 (2009) 3270-3278.
- [9] V. Baroghel-Bouny, G. Villain, M. Thiéry, T. Chaussadent, Durabilité du béton armé et de ses constituants : maîtrise et approche performantielle, Etudes et recherches des laboratoires des ponts et chaussées, 2008.
- [10] C. Alonso, C. Andrade, M. Castellote, P. Castro, Chloride threshold values to depassivate reinforcing bars embedded in a standardized OPC mortar, *Cement and Concrete Research*, 30 (2000) 1047-1055.
- [11] M.A. Pech-Canul, P. Castro, Corrosion measurements of steel reinforcement in concrete exposed to a tropical marine atmosphere, *Cement and Concrete Research*, 32 (2002) 491-498.
- [12] U.M. Angst, B. Elsener, C.K. Larsen, Ø. Vennesland, Chloride induced reinforcement corrosion: Electrochemical monitoring of initiation stage and chloride threshold values, *Corrosion Science*, 53 (2011) 1451-1464.
- [13] C. Cremona, L. Adélaide, Y. Berthaud, V. Bouteiller, V. L'Hostis, S. Poyet, J.-M. Torrenti, Probabilistic and predictive performance-based approach for assessing reinforced concrete structures lifetime: The applet project, in: K.P. V.L'Hostis, R.Gens and C.Gallé (Eds.) (Ed.) AMP 2010 – International Workshop on Ageing Management of Nuclear Power Plants and Waste Disposal Structures (EFC Event 334), EPJ Web of Conferences, Toronto, Ontario, Canada, 2011.
- [14] V. Bouteiller, C. Cremona, V. Baroghel-Bouny, A. Maloula, Corrosion initiation of reinforced concretes based on Portland or GGBS cements: Chloride contents and electrochemical characterizations versus time, *Cement and Concrete Research*, 42 (2012) 1456-1467.
- [15] C. Q. Li, Life-cycle modelling of corrosion-affected concrete structures: propagation, *Journal of Structural Engineering*, 129 (2003) 753-761.
- [16] S. Ahmad, Reinforcement corrosion in concrete structures, its monitoring and service life prediction—a review, *Cement and Concrete Composites*, 25 (2003) 459-471.
- [17] V. Bouteiller, J.-F. Cherrier, V. L'Hostis, N. Rebolledo, C. Andrade, E. Marie-Victoire, Influence of humidity and temperature on the corrosion of reinforced concrete prisms, *European Journal of Environmental and Civil Engineering*, 16 (2012) 471-480.
- [18] AFNOR, NF EN 206-1 / P18-325-1. Béton : spécification, performances, production et conformités, in, 2004.
- [19] H.S. So, S.G. Millard, On-site measurements on corrosion rate of steel in reinforced concrete, *ACI Materials Journal*, 104 (2007) 638-642.
- [20] M. Stern, A.L. Geary, Electrochemical polarization. I - A theoretical analysis of the shape of polarization curves, *Journal of Electrochemical Society*, 104 (1957) 56-65.

- [21] C. Andrade, J.A. González, Quantitative measurements of corrosion rate of reinforcing steels embedded in concrete using polarization resistance measurements, *Werkstoffe und Korrosion*, 29 (1978) 515-519.
- [22] C. Andrade, C. Alonso, RILEM TC 154-EMC:Electrochemical Techniques for Measuring Metallic Corrosion - Recommendations - Test methods for on-site corrosion rate measurement of steel reinforcement in concrete by means of the polarization resistance method, *Materials and Structures*, 37 (2004) 623-643.
- [23] NF EN ISO 8407, Corrosion of metals and alloys — Removal of corrosion products from corrosion test specimens, in, AFNOR, 2002.
- [24] D. Neff, S. Reguer, L. Bellot-Gurlet, P. Dillmann, R. Berthelon, Structural characterization of corrosion products on archaeological iron. An integrated analytical approach to establish corrosion forms, *Journal Raman Spectroscopy*, 35 (2004) 739-745.
- [25] C. Andrade, A. Castillo, Evolution of reinforcement corrosion due to climatic variations, *Materials and Corrosion*, 54 (2003) 379-386.
- [26] C. Andrade, C. Alonso, J. Sarria, Corrosion rate evolution in concrete structures exposed to the atmosphere, *Cement and Concrete Composites*, 24 (2002) 55-64.
- [27] K. Bhargava, A.K. Ghosh, Y. Mori, S. Ramanujam, Modeling of time to corrosion-induced cover cracking in reinforced concrete structures, *Cement and Concrete Research*, 35 (2005) 2203-2218.
- [28] D. Neff, J. Harnisch, B. Beck, V. L'Hostis, J. Goebbels, D. Meinel, Morphology of corrosion products of steel in concrete under macrocell and self-corrosion conditions, *Materials and Corrosion*, 62 (2011) 861-871.
- [29] V. L'Hostis, E. Amblard, W. Guillot, C. Paris, L. Bellot-Gurlet, Characterisation of the steel concrete interface submitted to chloride-induced-corrosion, *Materials and Corrosion*, 64 (2013) 185-194.